ISSN1027-5495. Functional Materials, 31, No.2 (2024), p. 185-191
doi:http://dx.doi.org/10.15407/fm31.02.185

The influence of aluminum on the morphological, optical properties and electronic structure of ZnO thin films

V.V.Zaika[1], N.K.Shvachko[1] , V.H.Kasiyanenko[2] , V.L.Karbivskyy[1], V.O.Moskaliuk[1], I.V.Sukhenko[1], A.P.Soroka[1]

[1]Kurdyumov Institute for Metal Physics of the National Academy of Sciences of Ukraine, 36, Vernadsky Blvd. Academician Vernadsky, 36, 03142 Kyiv, Ukraine
[2]Vinnytsia National Technical University, 95 Khmelnytske Shosse, Vinnytsia, Ukraine, 21021, Vinnytsia, Ukraine

Received February 23, 2024

Using radiofrequency magnetron deposition method, thin ZnO films modified with aluminum were obtained. The aluminum modification was carried out by placing aluminum plates with a size of 0.5x0.5 cm^2 on a zinc oxide target during the synthesis. The effect of aluminum substitution on the electronic, morphological, and optical properties of the thin films was studied. It is shown that the films have a developed surface with clusters of close to spherical shape. A change in the average size of the clusters, as well as an increase in the cluster size dispersion with increasing aluminum concentration was observed. X-ray photoelectron spectroscopy revealed that the binding energy of O 1s electrons decreases with increasing aluminum concentration, indicating an increase in the electron density on oxygen atoms. Spectrophotometric studies showed an increase in the transparency of the films in the visible and infrared ranges with increasing aluminum concentration. The optical spectroscopy method was used to estimate the band gap, which varies from 3.42 to 4.00 eV depending on the aluminum concentration.

Keywords: ZnO thin films, morphology, electronic structure, band gap, aluminum influence, transmission spectra, radiofrequency magnetron deposition.

Вплив алюмінію на морфологічні, оптичні властивості та електрону будову тонких плівок ZnO. *В.В.Заіка, Н.К. Швачко, В.Х. Касіяненко, В.Л. Карбівський, В.О.Москалюк, І.В.Суxенко, А.П. Сорока*

Методом радіочастотного магнетронного осадження отримані тонкі плівки ZnO з заміщеннями алюмінієм. Модифікація алюмінієм здійснювалось за рахунок розміщення алюмінієвих пластинок розміром 0.5x0.5 $см^2$ на мішені з оксидом цинку в процесі синтезу плівок. Досліджено вплив алюмінієвих заміщень на електронні, морфологічні та оптичні властивості тонких плівок. Показано, що плівки володіють розвиненою поверхнею з утвореннями кластерів форми близької до сферичної. Спостерігається зміна середнього розміру кластерів, а також збільшення дисперсії за розміром кластерів при збільшенні концентрації алюмінію. За допомогою методу рентгенівської фотоелектронної спектроскопії встановлено зменшення енергії зв'язку O 1s електронів зі збільшенням концентрації алюмінію, що свідчить про притік електронної густини до атомів кисню. Спектрофотометричні дослідження показали збільшення прозорості плівок у видимому та інфрачервоному діапазоні зі збільшенням концентрації алюмінію. Методом оптичної спектроскопії оцінена ширина забороненої зони, яка змінювалась від 3.42 до 4.00 еВ в залежності від концентрації алюмінію.

1. Introduction

ZnO thin films attract more attention due to their unique properties, in particular, a significant exciton binding energy (60 meV), good transparency in the visible and infrared spectral regions (>80%), as well as a band gap of 3.37 eV [1]. Therefore, this material can be used in various industries, namely in thin-film transistors, gas sensors, white LEDs, solar cells, and as piezoelectric semiconductors [2]. Low cost and environmental friendliness combined with high stability and easy availability make ZnO a promising material. ZnO thin films have many advantages over the industrially used indium tin oxide (ITO) as transparent conductive oxides. However, ZnO thin films are still inferior in transparency and electrical conductivity to ITO, and thus require further laboratory research to be implemented in industrial processes.

There are many synthesis methods for obtaining ZnO thin films, including sol-gel, chemical vapor deposition, spray pyrolysis, and magnetron deposition [3-5]. Among all methods, radiofrequency (RF-) magnetron deposition provides good film homogeneity on large-area substrates, low synthesis temperature, simplicity and scalability of the process. The deposition of thin films requires careful preparation of the target. The target can be created by pressing zinc oxide powder, which makes the synthesis process more flexible. Aluminum plates placed on a ZnO target (Fig. 1) make it possible to modify ZnO films with aluminum to obtain functional AZO films with desired characteristics. Laboratory studies are required to determine the physical properties of the resulting AZO films.

Many studies have been devoted to aluminum-substituted ZnO thin films obtained by RF-magnetron deposition. In [6], the effect of synthesis temperature on electrical, optical, and morphological properties was studied. There are works on the effect of magnetron deposition power, synthesis pressure, annealing, etc. on the obtained properties [7]. However, the effect of aluminum on the electronic structure of AZO thin films remains unclear. For example, in [8] it was shown that the O 1s spectrum differs significantly for films with an aluminum content of 10%, 15%, and 40%. This fact remains to be clarified. Also, in [9], the degree of aluminum oxidation was assessed using the XPS method, but the effect of aluminum on the electronic structure was not analyzed in detail. Thus, there is still a need for a detailed investigation of the effect of aluminum on the electronic structure of ZnO thin films.

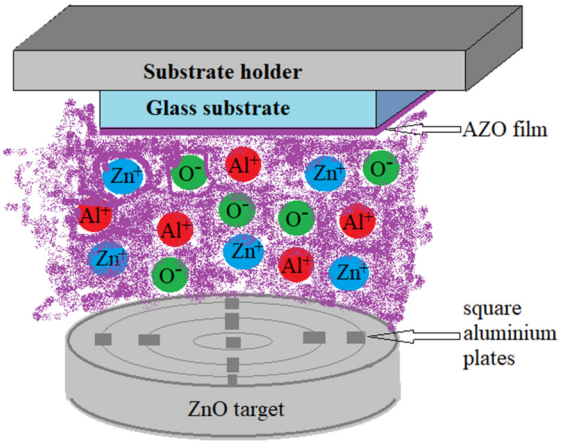

Fig. 1 Illustration of AZO thin film synthesis by RF-magnetron deposition

2. Experimental

ZnO thin films were deposited by RF-magnetron deposition (13.56±0.135 MHz) from a target with a diameter of 4.0 cm (12.57 cm^2) made from pressed ZnO powder of high purity (99.9%). For modification, Al (99.5%) was introduced in the form of squares with an area of 0.25 ± 0.05 cm^2, which were evenly distributed on top of the ZnO target (Fig. 1). A glass slide (1x1 cm^2) was used as a substrate, pre-cleaned with acetone and isopropyl alcohol in an ultrasonic bath for 20 minutes and washed with deionized water. After that, the glass was transported to a vacuum chamber and placed at a distance of 4.5 ± 0.1 cm above the ZnO target. A pre-vacuum pump and a nitrogen trap diffusion pump were used to obtain a high vacuum of $5.0 \cdot 10^{-5}$ Pa. Argon (99.9%) was used to produce the plasma. The pressure inside the chamber during deposition was $8 \cdot 10^{-1} \div 2 \cdot 10^{-2}$ Pa. The films were deposited at a magnetron power of 100±20 W. Aluminum doping was carried out by placing of aluminum plates on the ZnO target: 2, 4, and 9 plates for Al05, Al10, and Al25 samples, respectively (Table 1). The target was pre-evaporated for 10 minutes to clean its surface, and then the films were deposited during 60 minutes.

The surface morphology of the ZnO thin films was analyzed by scanning electron microscopy (SEM) using a Tescan Mira 3 microscope.

The XPS spectra of the the samples were obtained on a JEOL XPS 2400 X-ray spectrometer. The operating pressure during the experiment

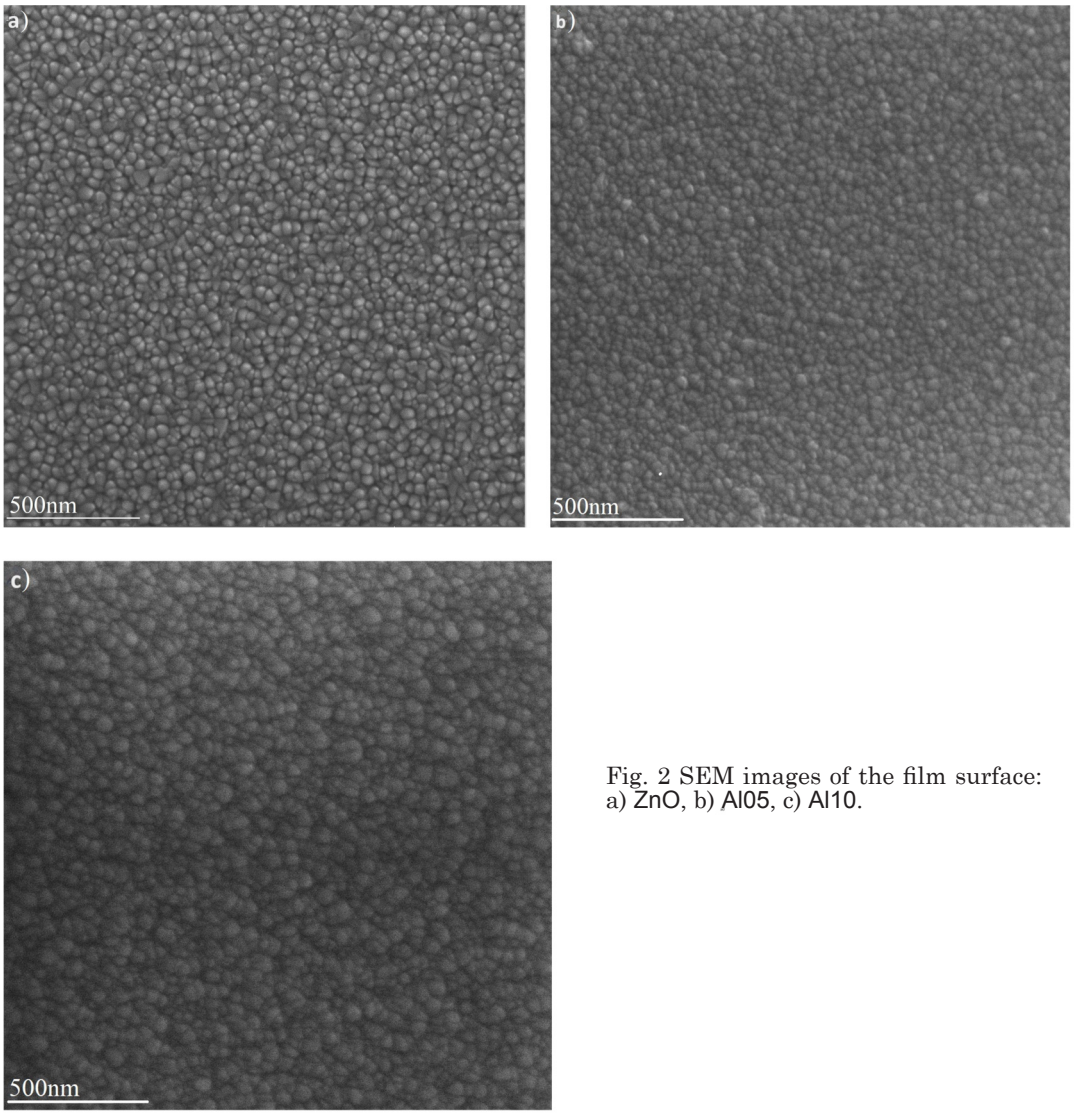

Fig. 2 SEM images of the film surface: a) ZnO, b) Al05, c) Al10.

was no more than $1.0 \cdot 10^{-7}$ Pa. The radiation of a magnesium anode with an energy of 1253.6 eV of the Mg Kα line was used. The energy resolution was 0.1 eV. During the imaging, the charging of the samples was not observed for ZnO, Al05, and Al10 films, with the exception of the Al25 sample. The charge correction was carried out using the C 1s line with an energy of 284.2 eV.

The optical transmission curves were obtained using a Spekol-1500 UV-vis-NIR spectrophotometer in the wavelength range of 190-1100 nm with a resolution of ±2 nm and an error in determining transparency of no more than 0.5%.

3. Results and discussion

SEM images of the surface of ZnO thin films were obtained. Figure 2 shows the characteristic morphology of the films with a developed surface consisting of almost spherical clusters. These clusters are densely packed and form a slightly textured surface. The films are fairly homogeneous without obvious foreign inclusions over a rather large area. The morphology of the surface changed slightly after aluminum modification. A comparison of SEM images of ZnO, Al05 and Al10 samples shows that with increasing aluminum concentration the average cluster size changes, as well as the cluster size dispersion**.** The average cluster sizes are approximately 34.0 ± 8.3, 31.6 ± 9.0, and 42.6 ± 11.0 nm for ZnO, Al05, and Al10 samples, respectively (Fig. 2). A detailed analysis reveals

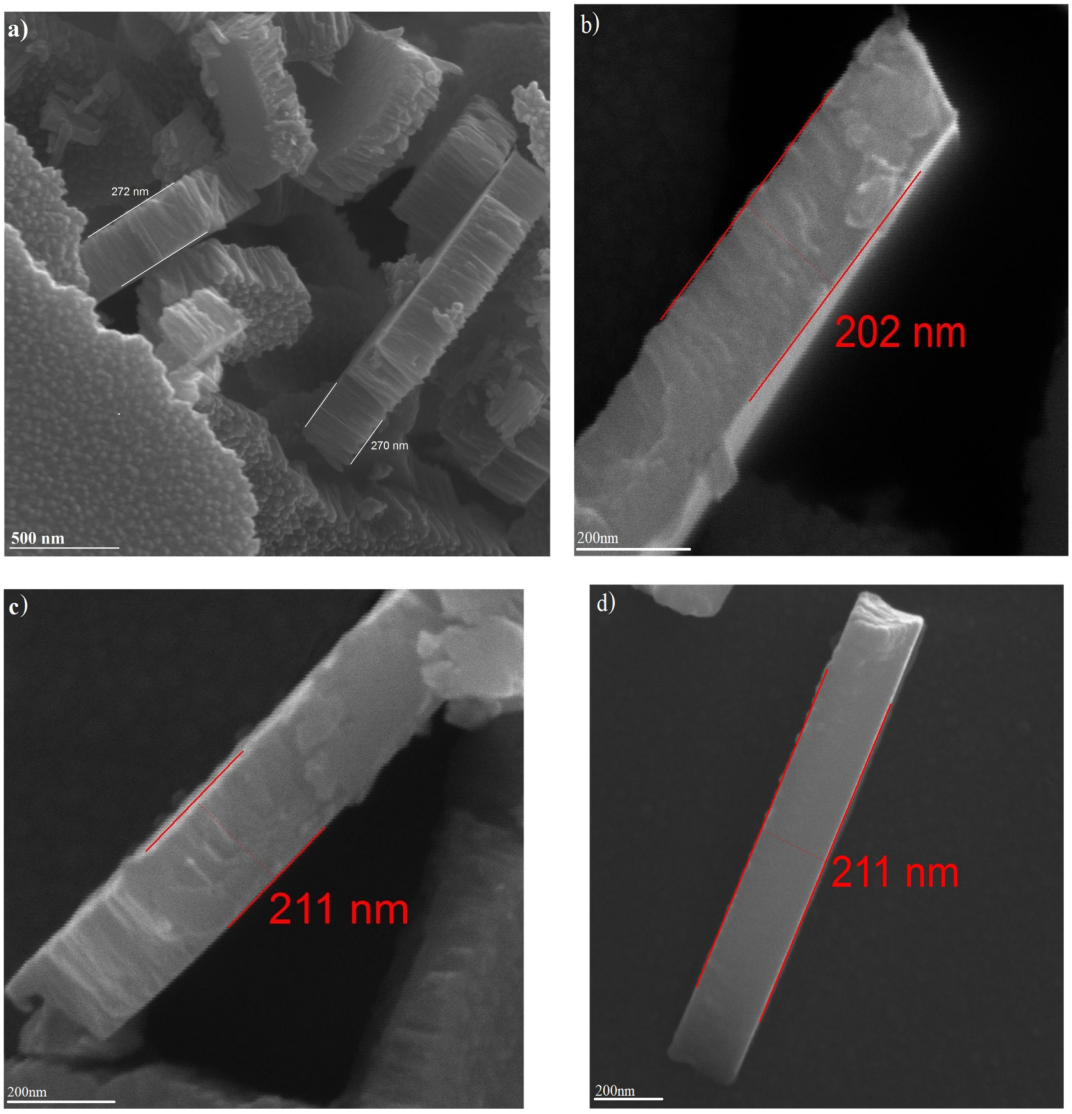

Fig. 3 Estimation of film thickness by SEM: a) ZnO, b) Al05, c) Al10, d) Al25.

an increase in the maximum size of some clusters with increasing aluminum concentration compared to the pure ZnO sample.

To assess the thickness of the samples, the surface of the films was scratched with a scalpel (Fig. 3). The film thickness was 270±5, 202±3, 211±5 and 211±3 nm for the ZnO, Al05, Al10 and Al25 samples, respectively (Fig. 3). To assess the uniformity of the film thickness over the area of the Al05 and Al10 samples, the film was torn in the middle and along the edges. In the Al05 sample, the film thickness was 200±4 nm at the edge and 220±3 nm in the middle. For the Al10 sample, the thickness at the edge was 210±4 nm, and in the middle – 242±7 nm. Thus, we can say that for the Al05 sample the thickness varies within 10%, and for the Al10 sample – within 20%. Considering the columnar growth of the films observed in Fig. 3, it can be argued that the films are polycrystalline and textured, and the polycrystals are oriented along the c-axis perpendicular to the substrate. Regarding film thickness, questions may arise about the influence of quantum size effects on the properties of ZnO thin films. Thus, in [10], thin ZnO films with a thickness of 2÷300 nm were obtained, and the authors observed a decrease in the band gap from 3.34 eV to 3.72 eV due to quantum size effects when going from films with a thickness of 21.3 nm to 4.7 nm. However, the difference between the band gap values for the 21.7 nm and 14.0 nm films did not exceed 0.05 eV. In another work [11], the results of ellipsometric studies show that

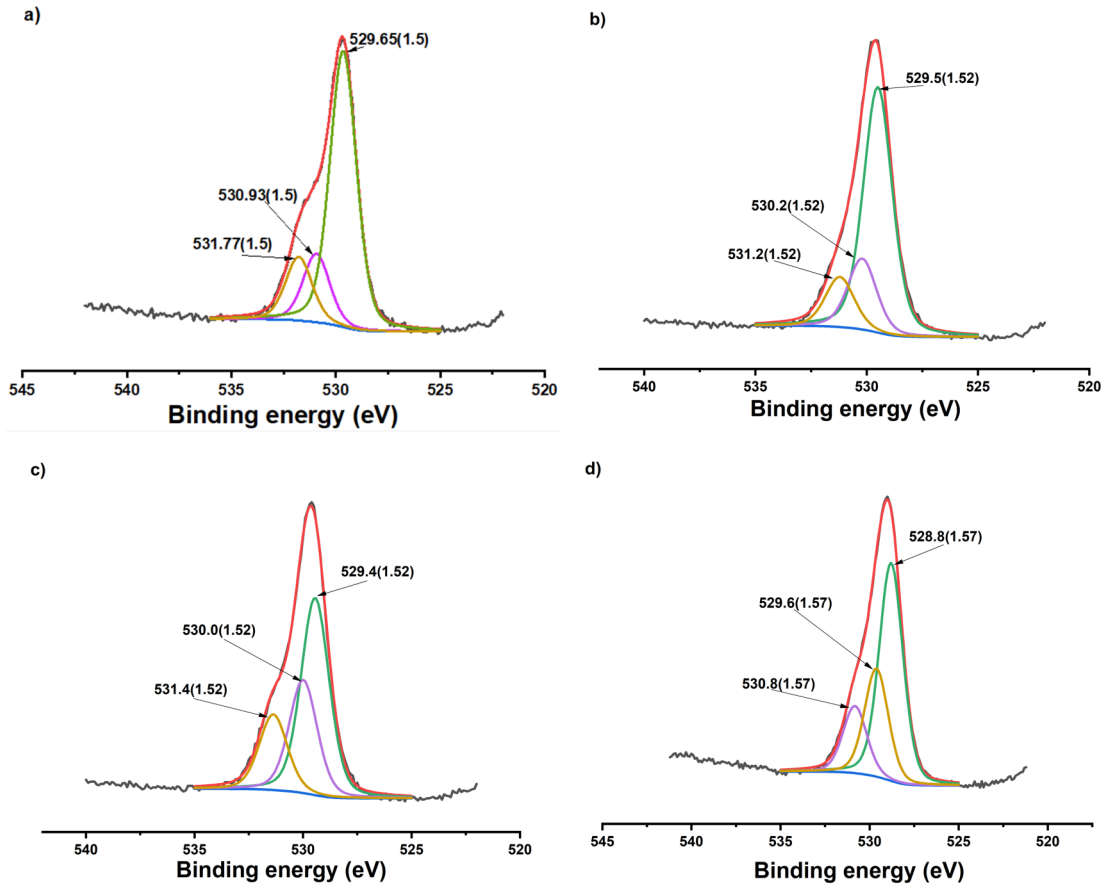

Fig. 4. XPS spectra of O1s level of thin films: a) ZnO, b) Al05, c) Al10, d) Al25.

quantum-size effects are clearly manifested for films with a thickness of less than 20.0 nm. Since the thicknesses of the films we obtained are equal to or greater than 200 nm, quantum size effects are insignificant or even absent.

To determine the electronic structure and chemical composition of the surface, XPS studies were performed. Quantitative chemical analysis was carried out over a wide spectrum by comparing the intensity of the Zn $2p_{3/2}$, O 1s, Al 2s peaks taking into account the photoionization cross section using the SpecSurf software (Table 2). The quantitative analysis shows that the atomic concentration of aluminum in AZO samples is higher than that estimated from the ratio of the areas of aluminum plates and the ZnO target during RF- magnetron deposition. The O 1s spectrum of oxygen was decomposed into 3 components (Fig. 4). The low-energy peak corresponds to O^{2-} ions in the ZnO matrix with a wurtzite structure with predominantly ionic Zn-O (or Al-O in the case of substitution) chemical bonds [12]. The middle peak belongs to O^{2-} ions in regions with oxygen deficiency in the ZnO matrix [13], or to oxygen in the surface

Table 1: Ratios of the areas of Al and ZnO targets used to obtain AZO films

Sample name	Slab area (cm^2)	Ratio of areas (%)
ZnO	0.0	0.00
Al05	0.5	3.98
Al10	1.0	7.96
Al25	2.5	19.89

layers. The high-energy peak is associated with adsorbed or chemically adsorbed forms of oxygen, namely O_2, CO, H_2O, or surface hydroxyl groups [14]. With increasing aluminum concentration, the binding energy of O1s decreases, indicating an increase in the electron density on oxygen atoms. This feature can be associated with both a larger number of valence electrons in the case of aluminum (3 vs. 2 in zinc) and with a lower electronegativity of aluminum on the Pauling scale.

Optical absorption spectra were obtained to determine the optical transparency of the films and the value of the band gap. The effect of aluminum doping on the optical properties of ZnO

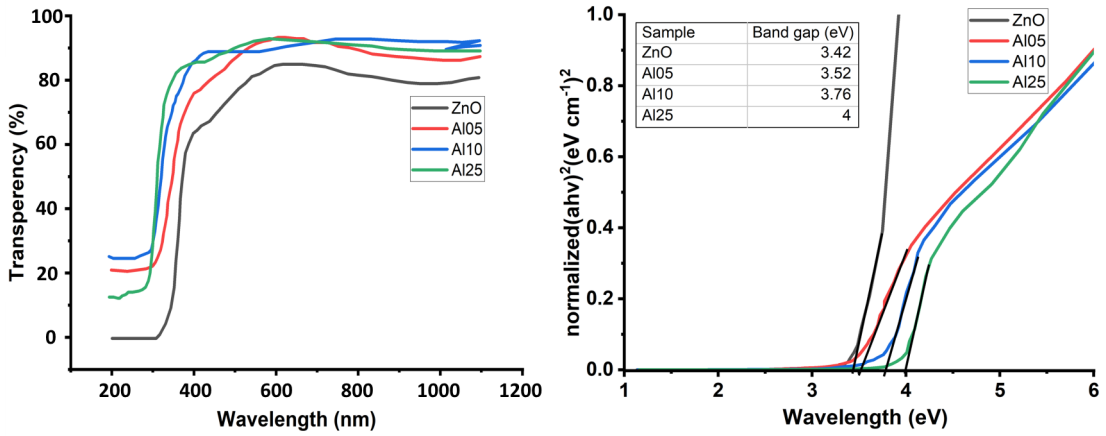

Fig. 5. a) Transmission spectra of ZnO thin films. b) Determination of the band gap by the Tauc method.

thin films has been studied. Fig. 5a shows the transmission spectra of ZnO films and films after their modification with aluminum. The best transparency of 93.6±0.5% was observed for the Al05 sample at a wavelength of 614±2 nm. It can be seen that all synthesized films have good transparency in the visible spectral range and strong absorption in the wavelength range below 400 nm, which is associated with the optical absorption edge. The sharp increase in absorption is associated with the energy of incident photons, which is sufficient to excite electrons from the occupied part of the valence band to free states in the conduction band. This also indicates that transparency increases with increasing aluminum concentration in the films. Consequently, these films can be used as functional UV protective coatings that require good transparency in the visible spectrum. The band gap was determined via the Tauc method [15] and is shown in Fig. 5b. The band gap increases from 3.42±0.02 to 4.00±0.02 eV with increasing aluminum dopant. The widening of the band gap can be explained by the fact that the states at the bottom of the conduction band are being populated by free electrons from aluminum, and as a result, the optical width increases: thus, the Moss-Berstein effect is observed [16, 17].

4. Conclusions

ZnO thin films modified with aluminum were synthesized by RF-magnetron deposition. The surface morphology studied by SEM shows the formation of clusters in the films with a shape close to spherical. A change in the average cluster size from 34.0 ± 8.3 nm to 42.6 ± 11.0 nm was detected with increasing aluminum concentration in the ZnO thin films. By scratching part of the film surface, its thickness was estimated to be 270±5 nm for pure ZnO and 202÷240±5 nm for samples with different degrees of Al doping. Spectrophotometric studies have shown that all the films have good transparency in the visible range, and transparency increases with increasing aluminum concentration. Also, with increasing aluminum concentration, an increase in the band gap from 3.42 ± 0.02 to 4.00 ± 0.02 eV was observed. Based on the results obtained, these films can be used as protective coatings against ultraviolet radiation.

Acknowledgment

We acknowledge financial support from the National Academy of Sciences of Ukraine (Project No. 6.8/24-P).

Table 2: Quantitative chemical analysis data

Sample	Element	Zn(at,%)	O(at, %)	Al(at,%)
ZnO		45.8±2.3	54.2± 2.7	-
Al05		49.0±2.5	51.0±2.6	-
Al10		48.2±2.4	51.8±2.6	-
Al25		31.6± 1.6	44.8±2.2	22.6±1.1

References

1. H. Liu, F. Zeng, Y. Lin, G. Wang, & F. Pan. *Applied Physics Letters, **102(18)**, 181908*, (2013).
2. S. Sharma, & C. Periasamy*, Superlattices and Microstructures, 73,* (2014).
3. L. Znaidi, *A review, **174(1-3)**, 18-30*, (2010).
4. S. Saini, P. Mele, T. Oyake, J. Shiomi, J.P Niemelä; M. Karppinen; K. Miyazaki, L. Chaoyang, K. Toshiyuki, A. Ichinose, L Molina-Luna*, Thin Solid Films, S0040609019303797*–, (2019).
5. A. K. Ambedkar, M.Singh, V. Kumar, V, Kumar, B. P. Kumar, A. Kumar, Y. K. Gautam. *Surfaces and Interfaces, **19**, 10050*, (2020).
6. Z. Zhang, C. Bao, W. Yao, S. Ma, L. Zhang, & S. Hou. *Superlattices and Microstructures*, ***49(6)**, 644–653,* (2011).
7. V. Şenay, *Journal of Materials Science: Materials in Electronics, **30**, 9910-9915*, (2019).
8. L. J. Li, H. Deng, L. P. Dai, J.J. Chen, Q. L. Yuan, & Y. Li, *Materials Research Bulletin, **43(6)**, 1456–1462, (2008).*
9. M.W. Alam, M.Z. Ansari, M. Aamir, et. al., *Crystals, **12(2)**, 128, (2022).*
10. A. Barnasas, N. Kanistras, A. Ntagkas, D.I. Anyfantis, A. Stamatelatos, V. Kapaklis, et. al, *Physica E: Low-Dimensional Systems and Nanostructures , **120**, 114072,* (2020).
11. D. Pal, J. Singhal, A. Mathur, A. Singh, S. Dutta, S. Zollner, S. Chattopadhyay, *Applied Surface Science, **421**, 341-348,* (2017).
12. R. Al-Gaashani, S. Radiman, A.R. Daud, N. Tabet, Y. Al-Douri, *Ceram. Int.*, **39**, No. 3: 2283–2292, (2013).
13. D. K. Kim and H.B. Kim, *J. Alloy. Compd,* **509**, No. 2: 421–425, (2011).
14. V.P. Singh and Ch. Rath, *RSC Adv.*, **5**, No.55: 44390–44397, (2015).
15. J. Tauc, *Mater. Res. Bull, **3(1)**, 37–46*, (1968).
16. T. S. Moss, *Proceedings of the Physical Society. Section B, **67(10)**, 775–782*, (1954).
17. E. Burstein, *Physical Review, **93(3)**, 632–633*, (1954).